Petroleum Science 19 (2022) 1853–1865

Contents lists available at ScienceDirect

Petroleum Science

journal homepage: www.keaipublishing.com/en/journals/petroleum-science

Original Paper

Study on the effect of CH_4 dissolution on the microstructure of wax crystal in waxy crude oil

Bing-Fan Li [a, b], Man-Ping Yang [a], Gang Liu [b, *], Li-Ming Zheng [a], Chao Yang [c]

[a] School of Vehicles and Energy, Yanshan University, Qinhuangdao, 066004, Hebei, China
[b] University of Petroleum (East China), Shandong Provincial Key Laboratory of Oil & GasStorage and Transportation Safety, Qingdao, 266580, Shandong, China
[c] Technology Inspection Center of Shengli Oilfield, SINOPEC, Dongying, 257000, China

ARTICLE INFO

Article history:
Received 20 October 2021
Received in revised form
8 April 2022
Accepted 11 April 2022
Available online 25 April 2022

Edited by Xiu-Qiu Peng

Keywords:
Waxy crude oil
CH_4 dissolution
Wax crystal
Rheology
Mechanism

ABSTRACT

In this work, the influence of the dissolution of methane (CH_4) gas on the wax crystal of waxy crude oil and the effect on the rheology of crude oil by dissolved CH_4 were studied comprehensively. A self-deign high-pressure micro visualization device was developed to analyze wax crystals before and after gas dissolution. The crude oil from Shengli and Nanyang was tested by the device under various gas pressures. Results showed that the viscosity, maximum shear stress and equilibrium shear stress of Shengli crude oil decreased with the increasing pressure of the dissolved CH_4. Due to the supersaturation of dissolved gas, the viscosity, maximum shear stress and equilibrium shear stress of Nanyang crude oil decreased initially and increased with the increasing pressure of dissolved CH_4. The change in rheology of the dissolved gas crude oil can be a combined influence of gas pressure and dissolution mechanisms caused by CH_4. Additionally, the wax precipitation point of Shengli crude oil decreased at the saturated dissolution of CH_4, while Nanyang crude oil showed an increasing wax precipitation temperature. Notably, the wax precipitation area, number of wax particles, and average diameter of wax crystal in both crude oils gradually decreased with dissolution. However, a saturation of CH_4 caused a small amount of precipitation of wax crystals in Nanyang crude oil, and the small wax crystals were aggregated to form the large wax crystals. The dissolution of CH_4 gas can affect the wax crystallization process, crystallization ability, and morphology of wax crystals that resulted in significant variation in the rheology of crude oil.

1. Introduction

During the production and transportation of crude oil, the precipitation and dissolution of volatile organic components can significantly affect the macro-rheological properties of crude oil and cause production problems (Yokozeki, 2007; Li et al., 2019a,b; Hinai et al., 2019; Hu et al., 2017). Recently, scholars (Yang et al., 2014.; Yu, 2009; Saboorian, 2012; Bank et al., 2017; Yang et al., 2012, 2013; Abivin et al., 2008) had been carried out a large number of experimental studies to explore the solubility of gases, pour point, viscosity, and other parameters of the dissolved gases in crude oil. Typically, with increasing pressure, the amount of dissolved gases gradually increases that caused a steady fall in the pour point, viscosity, and yield stress of crude oil before the saturation of crude oil. The gas dissolution can reduce the viscosity of crude oil. However, there was still a lack of understanding about the influence of CH_4dissolution on the wax crystals in waxy crude oil and the rheology change of crude oil caused by the micro mechanism of CH_4 dissolution.

In order to clarify the complex rheological mechanisms of waxy crude oil, a large number of studies based on microscopic characteristics of wax crystals of crude oil have been carried out. Cheng Chang et al. (2000) studied the effect of thermal history on microstructure and yield stress of wax crystals during static cooling. The results showed that the wax crystal particles gradually aggregated from irregular spherical particles into a chain structure, and finally formed a network structure. Garcia and Carbognani (2001) concluded that the asphaltenes acted as nucleation centers for waxes, and thus hastening the growth of the crystals and

* Corresponding author. No.66 of Changjiang West Road in Huangdao, Qingdao, China.
E-mail address: liugang@upc.edu.cn (G. Liu).

https://doi.org/10.1016/j.petsci.2022.04.007

shifting the WAT upward. Oliveira et al. (2007) studied the effect of asphaltene on wax crystal by optical microscope and found that with the incorporation of asphaltenes, the crystals were smaller and unevenly shaped. Jiaqiang Jing et al. (2008) proposed a fractal model to characterize the volume characteristics and fractal dimension of wax crystals. It was pointed out that increasing fractal dimension of wax crystal along with decreasing number of wax crystals can improve the low-temperature rheology of oil, though the effects of the dissolved gas were not included. Gang Liu et al. (2010) studied the rheology of waxy crude oil and showed that the fractal dimension is directly proportional to oil temperature and logarithmic function of the viscosity of crude oil. An innovative approach focusing on characteristic void length, proposed by Zhang (2011), was provided by quantitative description of wax crystals. By using several oil samples, it was confirmed that this parameter was correlated with the macro rheology of crude oil and can accurately characterize the distribution law of wax crystals. Yi and Zhang (2011) analyzed the fractal dimension of wax crystals of eight waxy crude oils treated with pour-point depressant by applying shear stress and the component characteristics of wax, resins, and asphaltene. They confirmed that at the temperature below the precipitation point of wax, shear stress can destroy the van der Waals force between wax particles, wax and asphaltene, wax and pour-point depressant, resulting in the damaged internal structure of crude oil and reduced fractal dimension. Hou et al. (2014) analyzed the microscopic images of wax crystals obtained from four waxy crude oils and verified that the diameter distribution of wax crystals followed the normal distribution, and the particle size distribution range was increased with increasing temperature. Bao et al. (2016) reported the effect of pre-shear rate on the rheology of gelled crude oil and found that a high pre-shear rate can cause a loss in angle, resulting in complex crystal structure with low yield value. Li et al. (2019a,b) studied the crystallization behavior of waxy crude oil from sol state to gel state. It was found that the smaller the cooling rate and the amount of wax crystal particles were, the larger the area and the more irregular shape of wax crystal were. Li et al. (2021) proposed a new method to observe the microstructure of wax crystals under dynamic cooling conditions with different shear rates, which improved the understanding of the microscopic information of gelled waxy crude oil.

Problems related to wax crystallization included wax deposition (Li et al., 2020; Agarwal et al., 2021; Yang et al., 2021), formation of gelled crude oil during shutdown (Magda et al., 2009; Fakroun and Benkreira, 2021) and the formation of Pickering emulsion (Liu et al., 2020; Yu et al., 2021; Chen et al., 2021). All these situations may lead to condensate accidents and huge economic losses, which highlighted the importance of understanding and addressing wax crystallization and related phenomena.

The previously reported studies had been focused to explore the microscopic characteristics of wax crystals under atmospheric pressure, and image processing technology had been used to quantitatively studies of wax crystals, but there were few studies on the influence of CH_4 dissolution on the wax crystal characteristics.

Therefore, considering that the microscopic observation of crude wax crystals in CH_4 atmosphere should not only ensure the sealing of the device, but also meet the visualization of the mesoscopic scale, and also need to consider the light transmittance of crude oil, a set of high-pressure microscopic visualization test device has been independently developed. The device was used to observe the wax crystal morphology of waxy crude oil with dissolved CH_4 dissolution, and the influence of CH_4 dissolution on the dynamic change law of wax crystal particles was analyzed from the morphological point of view. It included the following three aspects: (1) Control the specific cooling rate, observe the precipitation characteristics of wax crystals in crude oil with dissolved CH_4, and explore the influence of CH_4 dissolution on the wax crystallization process in crude oil; (2) Control the wax crystal in a stable initial crystallization state, and then change the pressure in the high-pressure microsystem, study the dynamic change laws of wax crystal particles in the process of CH_4 dissolution, and furthermore explore the influence mechanism of CH_4 dissolution on the internal wax crystal structure of crude oil; (3) Combined with the rheological test results and X-ray diffraction experimental results, study the influence mechanism of CH_4 dissolution on the rheology of waxy crude oil.

2. Experimental method and characterization

2.1. High-pressure microscopic visualization test device functioning

The high-pressure microscopic visualization test device was developed using the OlympusBX51 polarizing microscope produced by Olympus, Japan. The main body was composed of a high-pressure cold and hot bench, a temperature controller, a freezing instrument, freezing irrigation, and a loading platform, as shown in Fig. 1. The size of 55 × 55 × 23 mm^3 of the cold and hot bench, 16 mm diameter of the sample chamber, and the height of 2 mm were considered during the experiment. The cooling and heating bench was divided into upper and lower parts, respectively, to facilitate replacing of samples. It was sealed by four screws. The lower part of the cold and hot bench was connected to the light transmission hole, inlet and outlet of air, inlet and outlet of liquid nitrogen, electric heating wire, and temperature sensor. The upper part was connected with the observation window. The materials of the light transmission hole and observation window were sapphire chips, respectively, which can realize the observation of wax crystals under different pressure and temperature conditions. The high-pressure cold and hot test bench can accurately control the temperature of oil samples through the flow of liquid nitrogen and the temperature controller. The temperature range was controlled between -20 °C and 150 °C with an accuracy of ±0.2 °C. The high-pressure gas cylinder was attached to generate a pressurization system with a maximum pressure bearing capacity of 6 MPa by the hot bench. The gas pressure was controlled through a pressure-reducing valve with a control accuracy of ±0.1 MPa.

The image acquisition software was used to capture wax crystal images. The image analysis software (ImageJ) was employed to mainly extract data and counts the required parameters to realize the quantitative characterization of wax crystals (Huang and Wang, 2013).

Initially, in order to use high pressure cold and hot test bench, the sample chamber was tight to avoid air pass and sealed with oil. The inlet and outlet shutoff valve were opened and gas was injected into the chamber for exhaust, and then the air outlet shutoff valve was closed to pressurize the sample. In order to reduce the base temperature of the sample chamber, the freezing instrument was kept turn on, and the temperature during testing was controlled via electric heating wire. Finally, images of wax crystals were observed by controlling the stage translation regulating valve and microscope focusing operation.

In order to fully contact the oil sample with the gas to form saturated live crude oil, the microscope slide was modified, as shown in Fig. 2. The diameter of 14 mm and thickness of 1.1 mm of the slide together with a groove with 6 mm diameter and 0.1 mm depth was used. The design of depth was optimized to satisfy the transmittance of light of the oil sample. The oil sample was prepared by cleaning the slide with gasoline and wiping it with absorbent cotton. The slide was preheated and dried completely. A glass rod was used to drop the oil into the groove of the slide, and cover glass to remove extra oil in the groove was used to form a uniform liquid film.

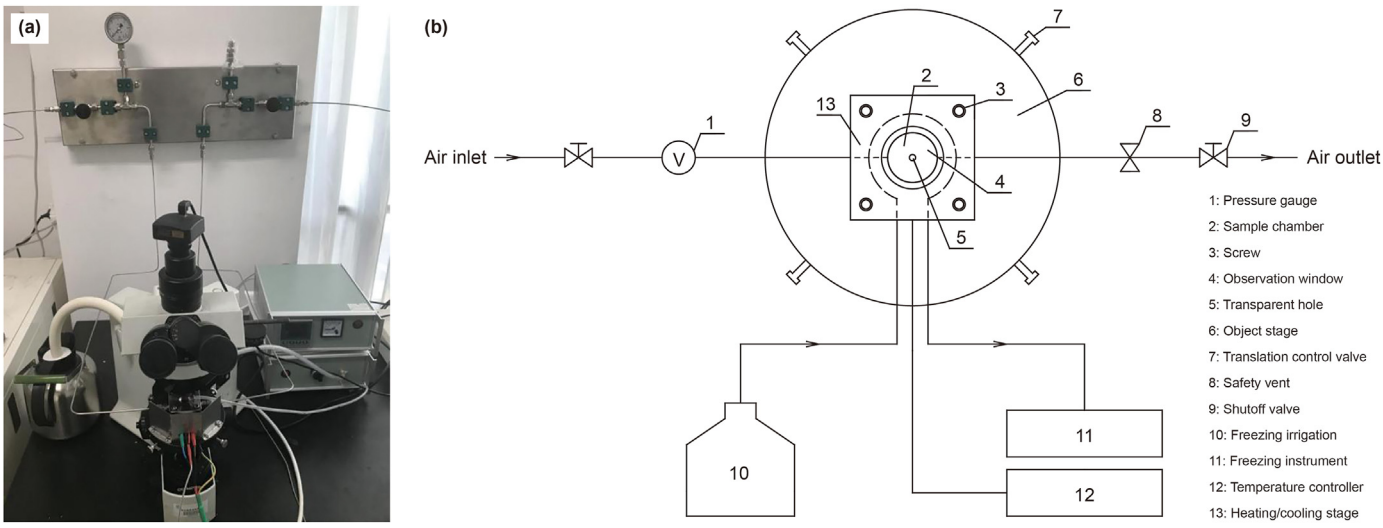

Fig. 1. High-pressure cold and hot test bench. (**a**) Physical map. (**b**) Schematic diagram.

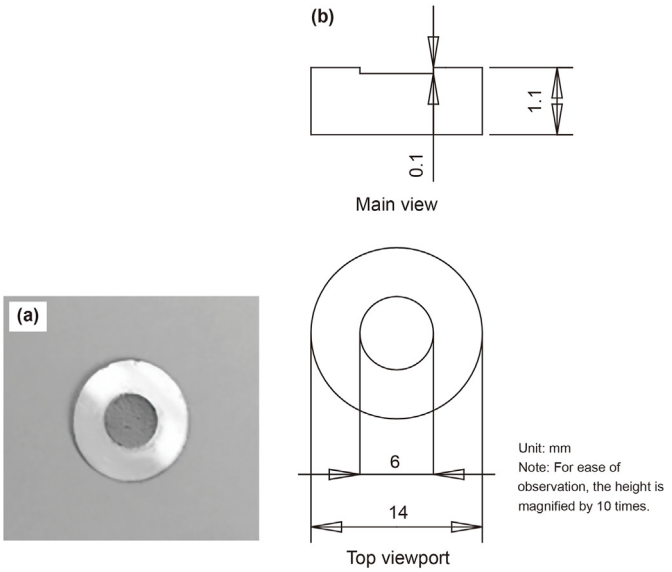

Fig. 2. Microscope slide of physical drawing and schematic diagram. (**a**) Physical map. (**b**) Schematic diagram.

2.2. Oil sample

The rheology of crude oil was affected by the content of wax, colloid and asphaltene. Therefore, due to the large differences content of wax, colloid and asphaltene, Shengli and Nanyang crude oil were selected as experimental samples. The pretreatment temperature of sample oil was 70 °C. The basic physical properties of oil samples under atmospheric pressure were shown in Table 1. The purity of 99.99% of CH_4 was utilized during the experiment.

2.3. Test scheme

To ensure the repeatability of the results obtained from microscopic and rheological tests, a pre-treatment was performed at 70 °C to eliminate the memory effect of shear and thermal history.

2.3.1. Rheological test

All samples were tested by MARS 60 high-pressure rheometer equipped with a closed pressure unit, air compressor, temperature control device, and attached software package. As shown in Fig. 3, the closed pressure unit was comprised of an external magnetic ring, internal magnetic ring, and measuring rotor body.

The viscosity and thixotropy of crude oil with dissolved CH_4 were measured by MARS 60 high-pressure rheometer.

(1) The pretreated oil sample was added to the pressure unit of the rheometer and heated to 70 °C. The pressure unit was scavenged and pressurized by CH_4. The test pressure of Shengli crude oil was 0 MPa, 1 MPa, 3 MPa and 5 MPa and the test pressure of Nanyang crude oil was 0 MPa, 1 MPa, 3 MPa, 4 MPa and 5 MPa, in which the oil samples was sheared in constant temperature for 2 h with the shear rate of 10 s^{-1}. In the process of CH_4 dissolution, CH_4 gas needed to be injected to maintain the constant pressure in the pressure unit. With the change of time, the pressure and viscosity of the pressure unit tended to be balanced. The two parameters remained unchanged within 2 h, indicating that the crude oil was saturated. After that, the crude oil was kept at a constant temperature for 20 min to eliminate the shear "memory" effect, and then the oil sample was cooled at a cooling rate of 0.5 °C/min during the cooling process of the oil sample, the constant shear rate (10 s^{-1}) was applied for dynamic cooling test.

(2) The pre-treated oil sample was added to the pressure unit and kept at a constant temperature of 70 °C for 20 min. Then, the oil sample was cooled to the test temperature (Shengli crude oil was cooled to 30 °C, Nanyang crude oil was cooled to 35 °C) at a cooling rate of 0.5 °C/min. Thereafter, the pressure unit was scavenged and pressurized by CH_4. The test pressure of Shengli crude oil was 0 MPa, 1 MPa, 3 MPa and 5 MPa and the test pressure of Nanyang crude oil was 0 MPa, 1 MPa, 3 MPa, 4 MPa and 5 MPa, in which the oil samples was sheared in constant temperature for 2 h with the shear rate of 10 s^{-1}. And then the crude oil viscosity was recorded.

(3) The pretreated oil sample was added to the pressure unit of the rheometer and heated to 70 °C. The pressure unit was scavenged and pressurized by CH_4. The test pressure of

Table 1
Basic physical properties of oil samples under atmospheric pressure.

Oil sample	Density (20 °C), kg/m^3	Pour point, °C	Wax content, %	Resins content, %	Asphaltene content, %
Shengli	878.2	34	24.5	18.03	0.12
Nanyang	875	47	38.2	–	15

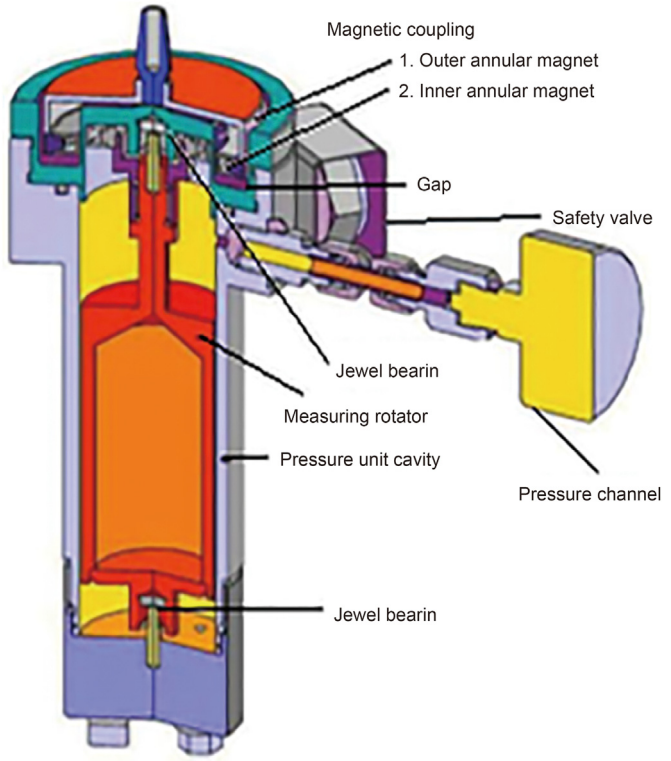

Fig. 3. Pressure unit for rheological testing.

Shengli crude oil was 0 MPa, 1 MPa, 3 MPa and 5 MPa and the test pressure of Nanyang crude oil was 0 MPa, 1 MPa, 3 MPa, 4 MPa and 5 MPa, in which the oil samples was sheared in constant temperature for 2 h with the shear rate of 10 s^{-1}. In the process of CH_4 dissolution, CH_4 gas needed to be injected to maintain the constant pressure in the pressure unit. With the change of time, the pressure and viscosity of the pressure unit tended to be balanced. The two parameters remained unchanged within 2 h, indicating that the crude oil was saturated. After that, the crude oil was kept at a constant temperature for 20 min to eliminate the shear "memory" effect, and then the oil sample was cooled to the test temperature (Shengli crude oil was cooled to 30 °C, Nanyang crude oil was cooled to 35 °C) at a cooling rate of 0.5 °C/min. After that, the constant shear rate (10 s^{-1}) shear test was carried out to obtain the thixotropic curve of crude oil.

2.3.2. Microscopic testing

The microscopic analysis of crude oil through a non-isothermal crystallization test was carried out. Initially, an oil sample was heated to 70 °C and added to a preheated microscope slide by glass rod to make the test piece. The test piece was kept into the high-pressure cooling and heating bench. The oil sample was heated to 70 °C, and the sample chamber was scavenged and pressurized by CH_4. The test pressure of Shengli crude oil was 0 MPa, 1 MPa, 3 MPa and 5 MPa and the test pressure of Nanyang crude oil was 0 MPa, 1 MPa, 3 MPa, 4 MPa and 5 MPa, in which a constant temperature for 2 h in order to get a complete dissolution of CH_4. Then, the oil sample was cooled to test temperature below the freezing point at a cooling rate of 0.5 °C/min. The precipitation characteristics of wax crystals in the crude oil under the condition of CH_4 dissolution were determined.

In order to examine the influence law of CH_4 dissolution on wax crystal particles, oil sample was prepared and kept at cooling and heating bench as mentioned above. The oil sample was heated to 70 °C and kept at a constant temperature for 20 min. Thereafter, an oil sample was cooled to the test temperature at a cooling rate of 0.5 °C/min and the sample chamber was scavenged and pressurized by CH_4. The test pressure of Shengli crude oil was 0 MPa, 1 MPa, 3 MPa and 5 MPa and the test pressure of Nanyang crude oil was 0 MPa, 1 MPa, 3 MPa, 4 MPa and 5 MPa. Each oil sample with dissolved CH_4 gas was continuously observed for 2 h, and the test results were recorded at the stable structure of the wax crystal.

2.3.3. X-ray test

After depressurization of oil samples, the XRD test was carried out by x'pert Pro MPD diffractometer to analyze lattice parameters of wax crystal before and after the CH_4 dissolution. The target Cu Kα X-ray at tube current of 40 mA and tube voltage of 40 kV was used for wide-angle diffraction i.e., $5° < 2\theta < 60°$. After the formation of saturated dissolved gas crude oil samples at variable gas pressure, the sampling was depressurized. Thereafter, an XRD test was conducted to analyze the wax crystal in each oil sample.

3. Results and discussion

3.1. Effect of CH_4 dissolution on rheology of waxy crude oil

Fig. 4 showed the viscosity - temperature curves of crude oil. Fig. 5 showed the thixotropic curve of crude oil. The variation trend of crude oil viscosity temperature curve and thixotropic curve under different dissolved gas pressure were similar to that under atmospheric pressure. With the decrease of temperature, the viscosity of the two crude oils increased gradually. Under the condition of constant shear rate, the shear stress decreased gradually and finally reached the dynamic equilibrium state.

In the range of test pressure, the viscosity, maximum shear stress and equilibrium shear stress of Shengli crude oil decreased with the increase of dissolved gas pressure. The viscosity, maximum shear stress and equilibrium shear stress of Nanyang crude oil decreased first and then increased with the increase of dissolved gas pressure. For dissolved gas crude oil, on the one hand, dissolved gas pressure led to the compression and aggregation of crude oil molecules as well as the enhancement of wax crystal interaction, which enhanced the structural strength of crude oil; On the other hand, with the gradual dissolution of CH_4, the tight cross-linking structure of wax crystals was destroyed, and the interaction between wax crystals was weakened, which weakened the structural strength of crude oil. The change of rheological property of gas dissolved crude oil was the result of the comprehensive influence of

gas dissolved pressure and gas dissolved amount. When the dissolved gas pressure was less than the bubble point pressure, the viscosity reducing effect of CH_4 played a leading role. When the dissolved gas pressure was greater than the bubble point pressure, the viscosity increasing effect of dissolved gas pressure played a leading role. In the range of test pressure (0–5 MPa, the pressure limit of the test instrument), with the increase of dissolved gas pressure, the change trend of viscosity curves and thixotropy curves of the two crude oils were inconsistent, which were caused by the phenomenon of gas supersaturation, and the bubble point pressure of Shengli crude oil was not reached under the test pressure.

3.2. Effect of CH_4 dissolution on non-isothermal crystallization of crude oil

Fig. 6 showed the surface morphology of wax crystals obtained from Shengli crude oil with respect to temperature at the dissolved gas pressure of 1 MPa. Initially, the wax molecules were completely dissolved in the liquid crude oil, and no wax crystals were precipitated in the crude oil (Fig. 6a) due to high oil temperature than that of wax precipitation point temperature (46.8 °C). As shown in Fig. 6b, when the oil temperature dropped to 46.8 °C, trace wax crystals started to precipitate in the crude oil, which can be notified as to the wax precipitation temperature of Shengli crude oil. Further decrease in temperature (45 °C) caused increasing number and size of wax crystals. The shape of wax crystals were mostly followed a regular circle, and the distribution of wax crystals was relatively dispersed and devoid of cross-linking between wax crystals. Meanwhile, the crude oil showed the characteristics of a Newtonian fluid, though the existence of solid particles in crude oil creates the deviation in fluid streamline (Li, 2007), which effectively reduced the fluidity of crude oil. At the oil temperature below 40 °C, the formation of wax crystals increased sharply, and the diameter of wax crystals increased gradually which caused irregularity in shape, resulting in weaken fluidity of crude oil. Subsequently, the wax crystals were cross-linked and aggregated with each other to form large round, flake, and rod-type wax crystal particles and furthermore formed a network structure, showing the characteristics of non-Newtonian fluid (Fig. 6d~f).

By using microscopic observation, the wax precipitation point temperatures of Shengli crude oil under the different dissolved gas pressure were recorded to 47.6 °C, 46.8 °C, 46.1 °C, and 45.3 °C, respectively. Similarly, the wax precipitation point temperatures of Nanyang crude oil were 57.8 °C, 55.9 °C, 53.2 °C, 53.8 °C, and 54.6 °C, respectively. With increasing gas pressure, the wax precipitation point of Shengli crude oil gradually decreased, while it decreased slowly up to 3 MPa and increased at 5 MPa for Nanyang crude oil. Specifically, the CH_4 dissolution increased the distance between oil molecules and improved the solubility of crude oil to wax. On the other hand, the existence of CH_4 molecules hindered the formation of wax crystals and reduced the wax precipitation point of dissolved gas crude oil. The dissolved gas pressure led to compression and aggregation of crude oil molecules, resulting in a decrement in the solubility of wax molecules in liquid oil, and consequently the wax precipitation point temperature of crude oil increased.

The characteristic parameters of wax crystal by means of wax precipitation area, number of particles, average diameter, and roundness of particles were obtained to realize the quantitative analyses of wax crystals. Fig. 7 showed the surface morphology of wax crystals with respect to the different dissolved gas pressures during non-isothermal crystallization. Table 2 showed the crystal structure parameters of wax crystals under the different dissolved gas conditions. It can be seen from Table 2 and Fig. 8 that with the increase of dissolved gas pressure, the wax crystallization area of Shengli crude oil decreased exponentially, the number of particles decreased linearly, the average diameter of particles decreased in quadratic function, and the roundness increased linearly. With the increase of dissolved gas pressure, the wax crystallization area, number of particles and average particle diameter of Nanyang crude oil decreased linearly, and the roundness increased linearly. With the further increase of dissolved gas pressure, the wax crystallization area, the number of particles and the average diameter of particles of Nanyang crude oil increased linearly, and the roundness decreased linearly. The composition of crude oil affected the effect of CH_4 on crude oil wax crystal.

The fitting results of apparent viscosity of crude oil and wax crystal structure parameters were shown in Fig. 9. Table 3 showed the main diffraction peak data in XRD before and after gas dissolution in crude oil. The apparent viscosity of Shengli crude oil increased in quadratic function with the increase of wax crystallization area, while the apparent viscosity increased linearly with the increase of the number of wax crystal particles, the average diameter of particles and the decrease of roundness. With the increase of wax crystallization area, the number of wax crystal particles, the average diameter of particles and the decrease of

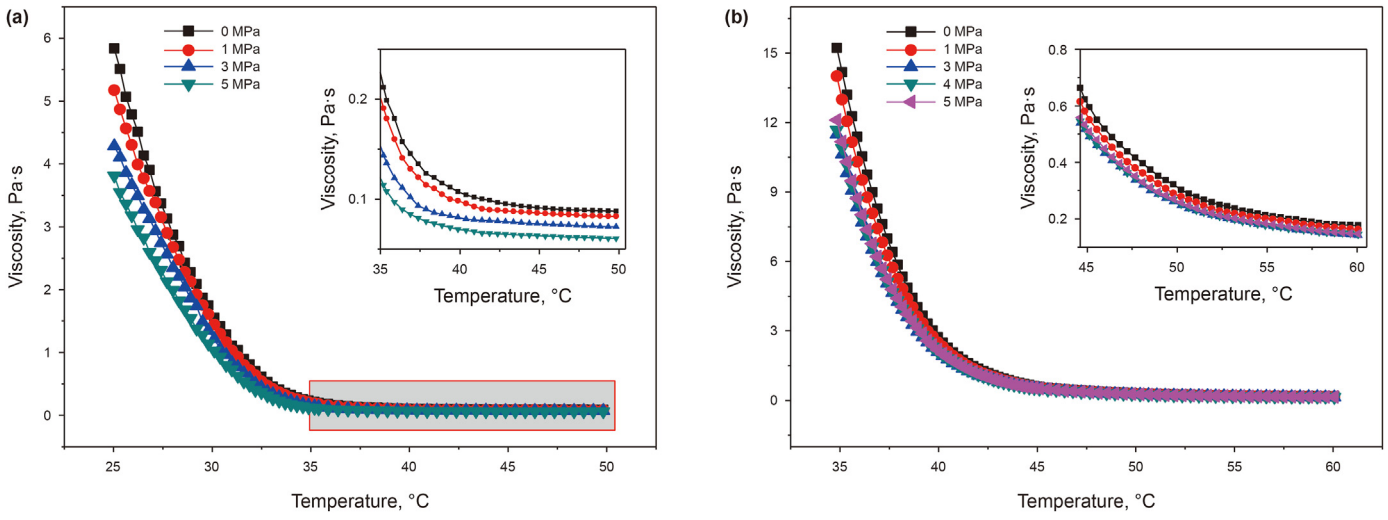

Fig. 4. Viscosity - temperature curve of crude oil. (**a**) Shengli crude oil. (**b**)Nanyang crude oil.

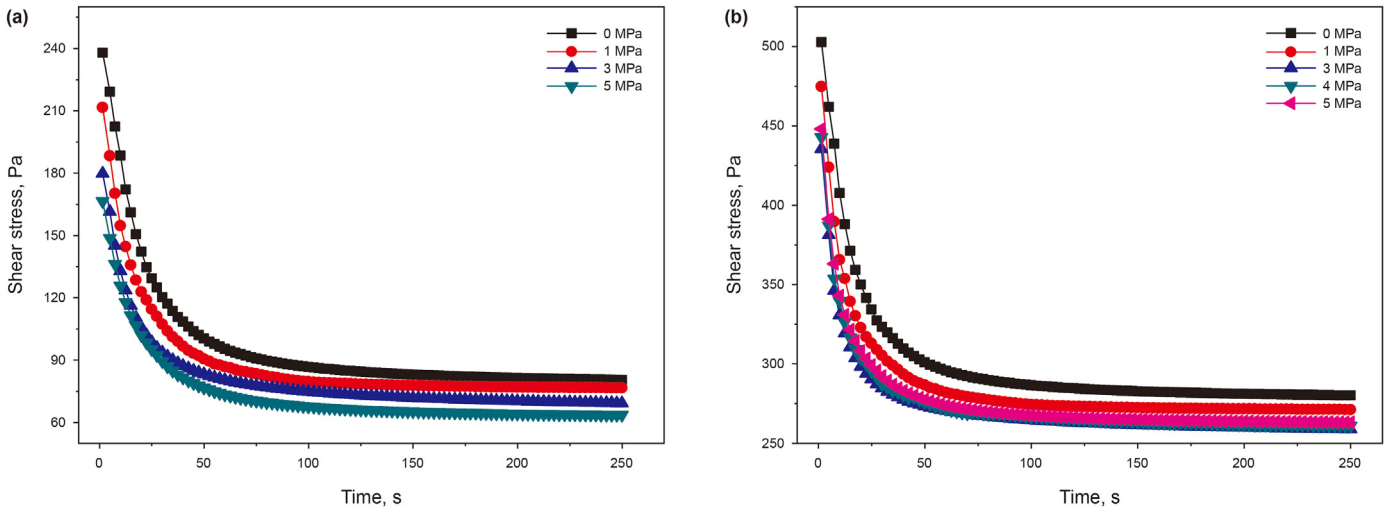

Fig. 5. Thixotropic curve of crude oil. (**a**) Shengli crude oil. (**b**) Nanyang crude oil.

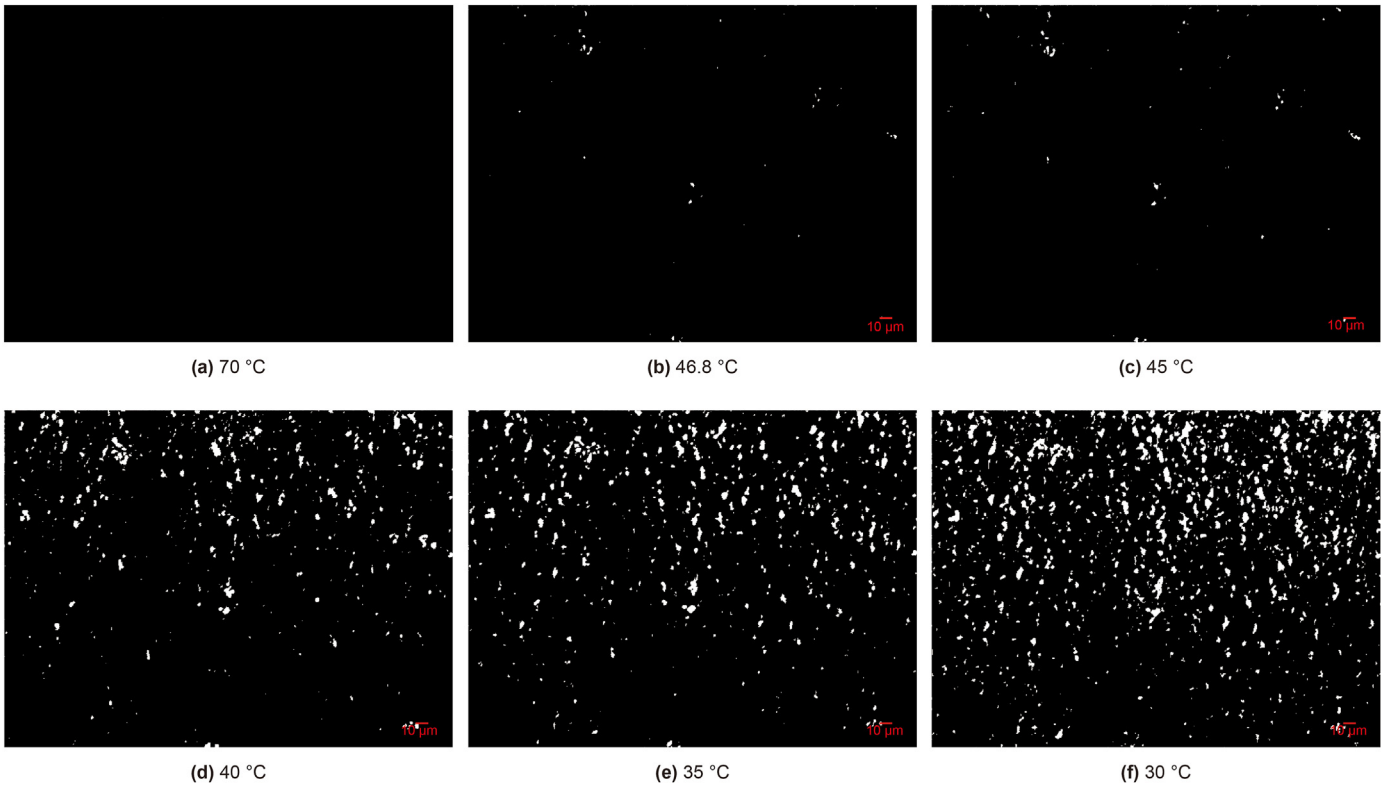

Fig. 6. Surface morphology and structure of wax crystal in Shengli crude oil at the dissolved gas pressure of 1 MPa at different temperatures. (**a**) 70 °C. (**b**)46.8 °C. (**c**) 45 °C. (**d**)40 °C. (**e**) 35 °C. (**f**)30 °C.

roundness, the apparent viscosity of Nanyang crude oil increased linearly. On the contrary, the apparent viscosity of Shengli crude oil decreased linearly.

The XRD patterns of Shengli and Nanyang crude oil before and after gas dissolution were shown in Fig. 10. The main diffraction peak data of the two oil samples were shown in Table 3.

It can be seen from Fig. 10 and Table 3 that the diffraction peaks of the two crude oils before and after CH_4 dissolution showed subtle change, confirming stability in the composition of wax crystal before and after gas dissolution. The interplanar spacing between the wax crystals of the two crude oils was decreased, indicating that the wax crystals possessed a compact network. During the crystallization process, the liquid oil can be separated from the crystal lattice of the wax crystal, which was beneficial to the fluidity of crude oil. Meanwhile, the intensity of the main diffraction peak and integral intensity of the wax crystal was significantly reduced, indicating a damaged crystal plane and a reduced particle size of the wax crystal during the growth process.

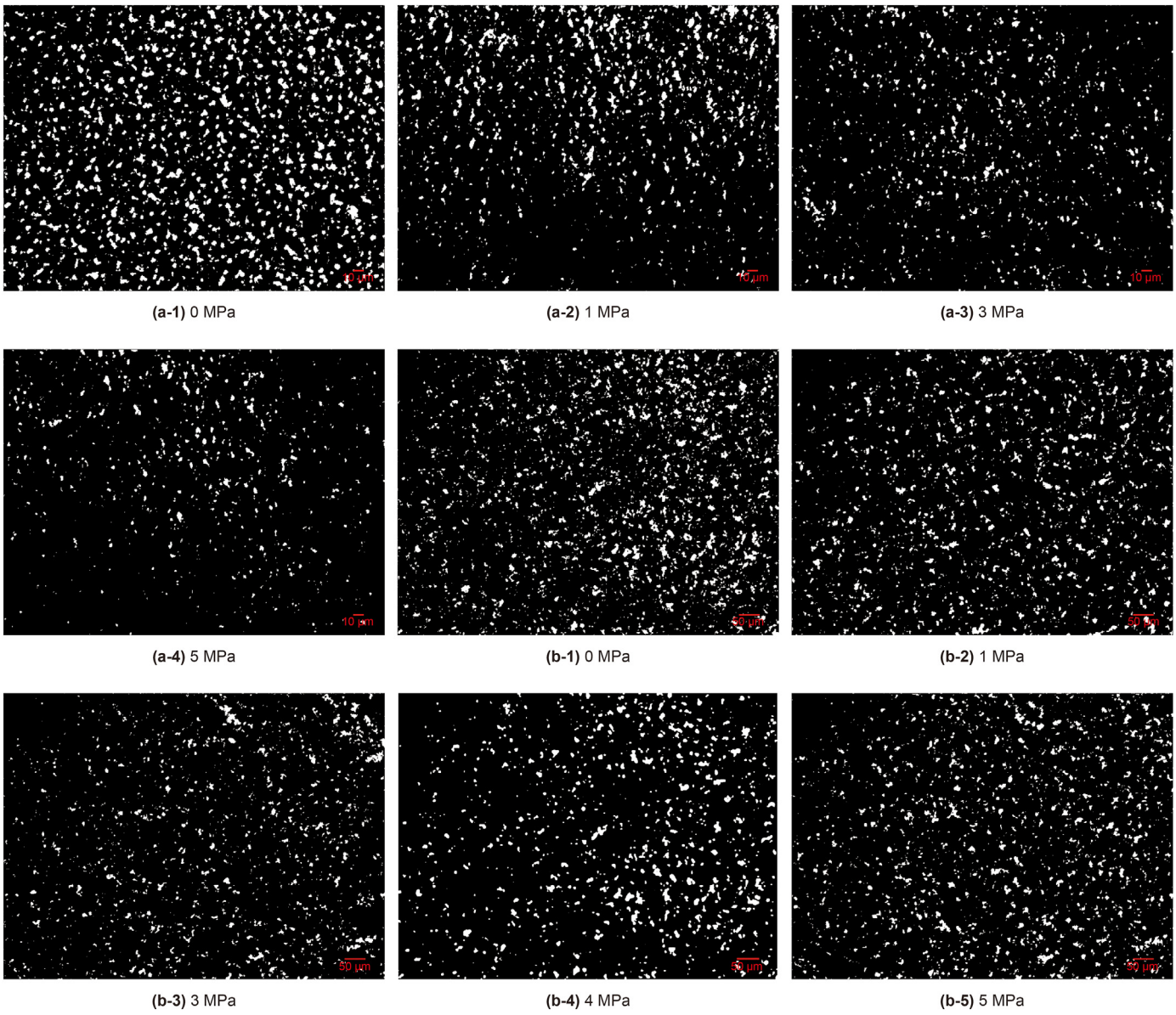

Fig. 7. a Images of Shengli crude oil wax under different dissolved gas pressure (30 °C). (**a-1**) 0 MPa. (**a-2**)1 MPa. (**a-3**) 3 MPa. (**a-5**)5MPa **b** Images of Nanyang crude oil wax under different dissolved gas pressure (35 °C). (**b-1**) 0 MPa. (**b-2**)1 MPa. (**b-3**) 3 MPa. (**b-4**)4 MPa. (**b-5**)5 MPa.

Table 2
Wax crystal structure parameters and viscosity at shear rate of 10 s^{-1} of crude oil under different dissolved gas pressure.

Oil sample	Pressure, MPa	Wax precipitation area, %	Number of particles	Average diameter of particles, um	Roundness	Apparent viscosity, Pa·s
Shengli (30 °C)	0	18.12	1415	3.798	0.826	1.552
	1	9.12	1131	3.163	0.832	1.442
	3	5.59	1025	2.478	0.845	1.216
	5	3.78	792	2.318	0.853	1.023
Nanyang (35 °C)	0	8.69	2078	3.069	0.848	15.217
	1	7.84	1907	3.043	0.855	14.008
	3	6.17	1581	2.965	0.880	11.489
	4	6.48	1654	2.971	0.870	11.675
	5	6.78	1695	3.002	0.861	12.110

The integral intensity of the diffraction intensity of plane 110 (peaking at 22°) before and after CH_4 dissolution in both crude oils was greater than that of plane 200 (peaking at 24°), indicating the density of plane 110 and the size of wax crystal decreased greatly, which can be conducive to improve the low-temperature fluidity of crude oil. Moreover, it can be confirmed that the CH_4 dissolution

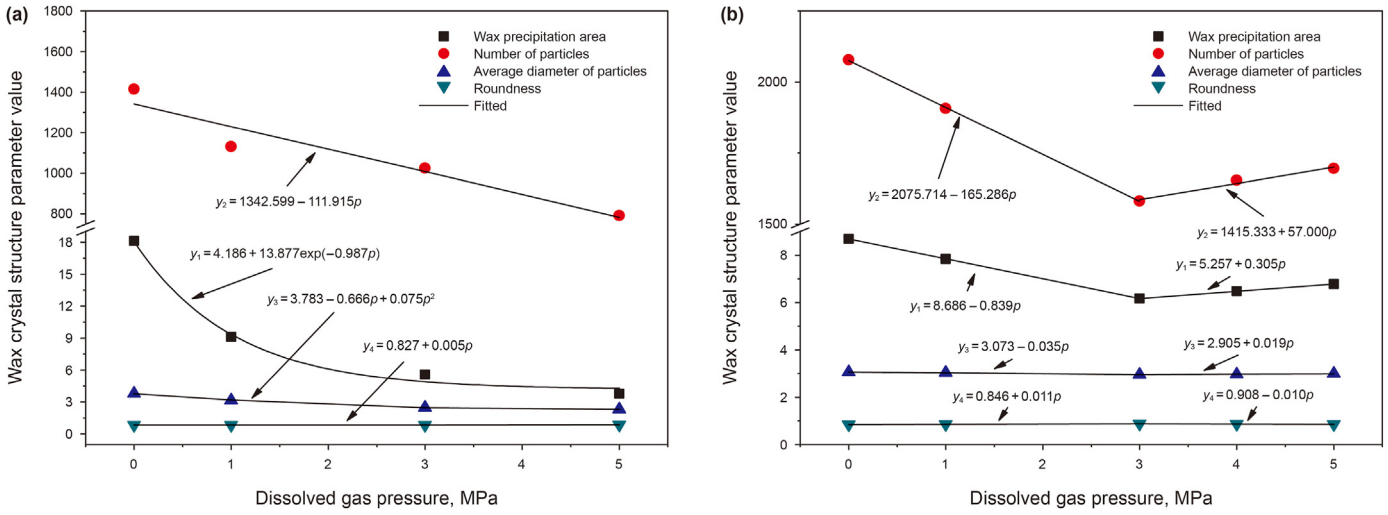

Fig. 8. Relationship between wax crystal structure parameters and dissolved gas pressure. (**a**) Shengli crude oil. (**b**) Nanyang crude oil.

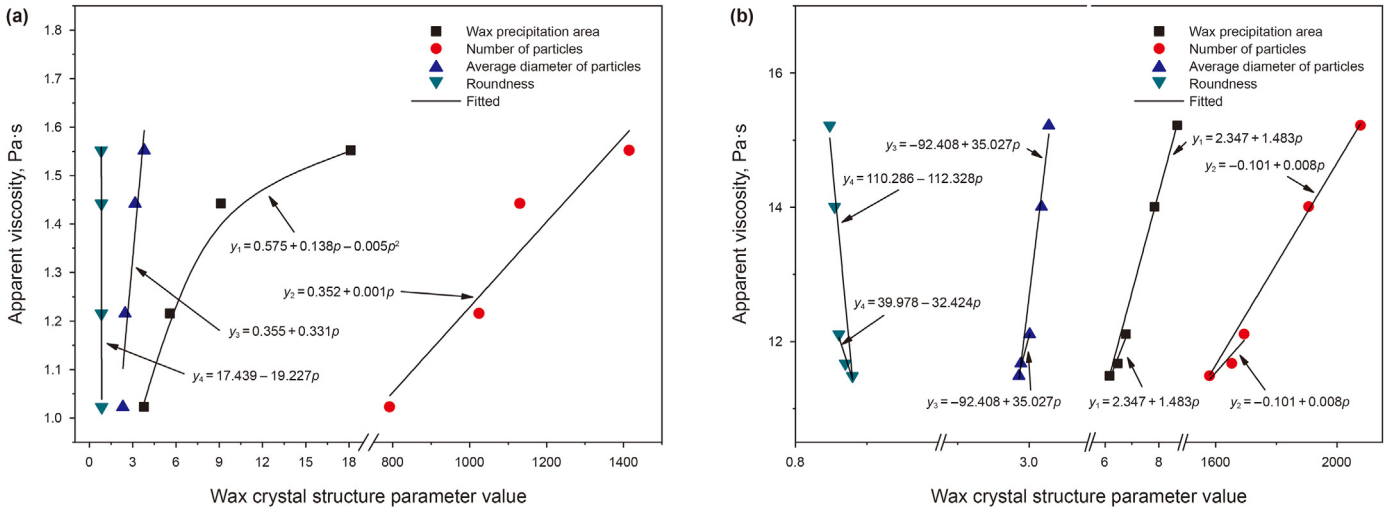

Fig. 9. Relationship between wax crystal structure parameters and apparent viscosity. (**a**) Shengli crude oil. (**b**) Nanyang crude oil.

Table 3
Main diffraction peak data in XRD before and after gas dissolution in crude oil.

Oil sample	2θ/°		Interplanar spacing/nm		Diffraction peak intensity/CPS		Integral strength	
	Degassed crude	Dissolved gas crude oil	Degassed crude	Dissolved gas crude oil	Degassed crude	Dissolved gas crude oil	Degassed crude	Dissolved gas crude oil
Shengli	21.34	21.34	4.17	4.15	15380	11898	60421	25401
	23.76	23.76	3.75	3.74	6287	5611	9585	4179
	35.96	35.95	2.50	2.49	1982	1919	2599	2244
Nanyang	21.36	21.36	4.16	4.15	16930	9384	137120	20103
	23.73	23.72	3.75	3.74	6846	3954	13324	3056
	35.96	35.96	2.50	2.49	1580	1402	2762	580

changed the crystallization process, crystallization ability of wax as well as morphology of wax, and consequently affected the rheology of crude oil.

3.3. Effect of CH_4 dissolution on wax crystals

The wax crystals in crude oil at a stable initial crystallization state were controlled. The influence laws of wax crystal particles under the condition of CH_4 dissolution were studied by changing the pressure in the high-pressure microsystem, and the related mechanisms of CH_4 dissolution on the crystal structure in crude oil were explored.

Fig. 11 showed the morphology of wax crystals obtained from Shengli and Nanyang crude oil, respectively, under the different dissolved gas pressures. Table 4 was the wax crystal structure parameters and viscosity at 10 s^{-1} of crude oil under different

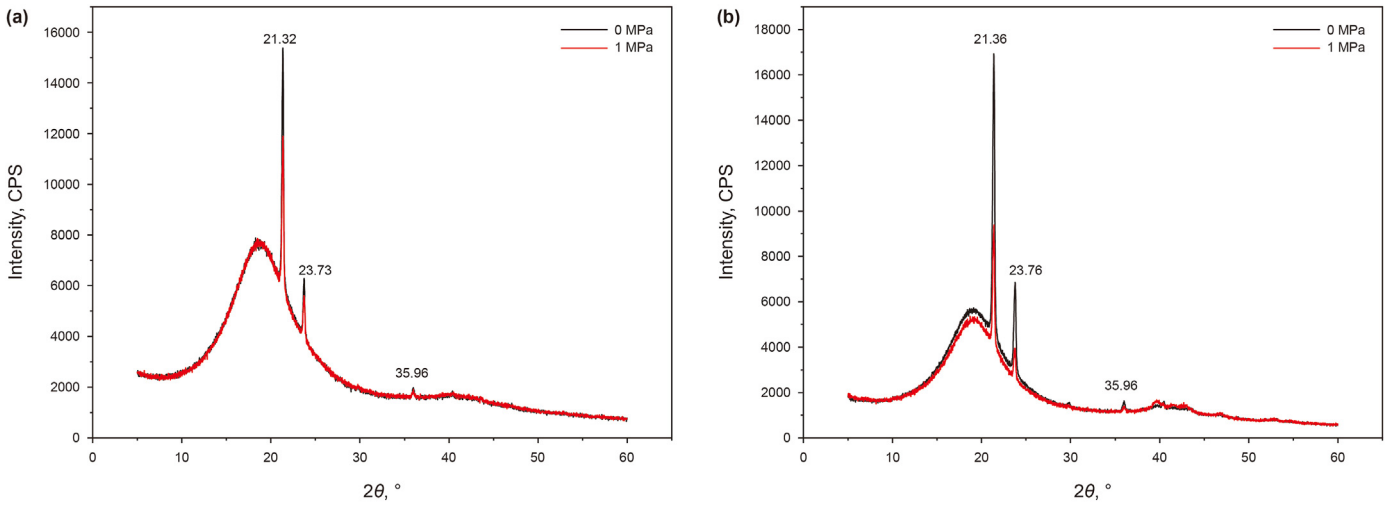

Fig. 10. X-ray diffraction results before and after gas dissolution in crude oil. (**a**) Shengli crude oil. (**b**) Nanyang crude oil.

dissolved gas pressure. Fig. 12 showed the relationship between wax crystal structure parameters and dissolved gas pressure. Due to the CH_4 dissolution, the original stable wax crystal structure was destroyed, and a small number of wax crystals began to fall off and gradually dissolved in liquid crude oil. The CH_4 dissolution caused a steady decrease in the wax crystallization area, number of wax crystals, and average diameter of particles. Further increment in gas pressure made saturation of the dissolved CH_4 that enhanced precipitation in Nanyang crude oil and a small number of wax crystals were formed (Fig. 11B(c ~ e)). The aggregation in wax crystals resulted in a bigger size of the wax crystals. It can be seen from Table 4 and Fig. 12 that with the increase of dissolved gas pressure, the wax crystallization area of Shengli crude oil decreased exponentially, the number of particles decreased linearly, the average diameter of particles decreased in quadratic function, and the roundness increased linearly. With the increase of dissolved gas pressure, the wax crystallization area, number of particles and average particle diameter of Nanyang crude oil decreased linearly, and the roundness increased linearly. With the further increase of dissolved gas pressure, the wax crystallization area, the number of particles and the average diameter of particles of Nanyang crude oil increased linearly, and the roundness decreased linearly. The compositions of crude oil affected the effect of CH_4 on crude oil wax crystal.

The fitting results of apparent viscosity of crude oil and wax crystal structure parameters were shown in Fig. 13. The apparent viscosity of Shengli crude oil increased quadratic function with the increase of wax crystallization area, while the apparent viscosity increased linearly with the increase of the number of wax crystal particles, the average diameter of particles and the decrease of roundness. With the increase of wax crystallization area, the number of wax crystal particles, the average diameter of particles and the decrease of roundness, the apparent viscosity of Nanyang crude oil increased linearly. On the contrary, the apparent viscosity of Shengli crude oil decreased linearly.

From the experimental point of view, it was impossible to independently investigate the influence of methane gas dissolution on the rheology of crude oil, because there must be dissolved gas pressure to dissolve methane gas in crude oil. Through the observation of wax crystals and the quantitative description of wax crystals, it was found that, on the one hand, the pressure of dissolved gas led to the compression and aggregation of crude oil molecules, resulting in decreasing solubility of wax molecules in liquid and precipitated wax crystals. On the other hand, due to the CH_4 dissolution, the ability of crude oil to dissolve wax crystals can be improved, making wax crystals dissolve gradually. Hence, the wax precipitation area, number of wax particles, and average diameter of particles gradually decreased, while the roundness in the shape increased. The quasi spheroidization of the shape of the wax particles reduced the surface area and surface energy of wax crystal particles that weakened the ability to adsorb and link the surrounding wax crystal particles. Thus, the flocculation ability of wax crystal flocs and the ability to form a spatial network structure were reduced. The quasi spheroidization of the shape of wax crystal particles reduced the surface area and surface energy of wax crystal particles, weakened the ability to adsorb and link the surrounding wax crystal particles, as well as the flocculation ability of wax crystal flocs and the ability to form spatial network structure. Therefore, the apparent viscosity of waxy crude oil decreased due to the quasi spheroidization shape of wax crystal. The reduction of effective internal phase volume fraction and the weakening of flocculation capacity of wax crystal flocs occurred due to the CH_4 dissolution.

XRD scanning experiments were carried out on Shengli and Nanyang crude oil before and after gas dissolution by X-ray diffractometer, as shown in Fig. 14. The main diffraction peak data of the two oil samples were shown in Table 5.

It can be seen from Fig. 14 and Table 5 that the diffraction peaks of the two crude oils before and after CH_4 dissolution showed subtle change, confirming stability in the composition of wax crystal before and after gas dissolution. At the same time, the main diffraction peak intensity and integral intensity of the wax crystal are significantly reduced, indicating that the crystal plane of the wax crystal is damaged and the particle size of the wax crystal becomes smaller during the growth process. The integral intensity of the diffraction intensity of the 110 plane (diffraction peak near 22°) before and after the gas dissolution of the two crude oils is greater than that of the 200 plane (diffraction peak near 24°), indicating that the crystal plane density of the 110 plane decreases more and the size decreases more, which is more helpful to improve the low-temperature fluidity of the crude oil. It can be concluded that the dissolution of CH4 changes the crystallization ability and wax crystal morphology, and then affects the rheology of crude oil.

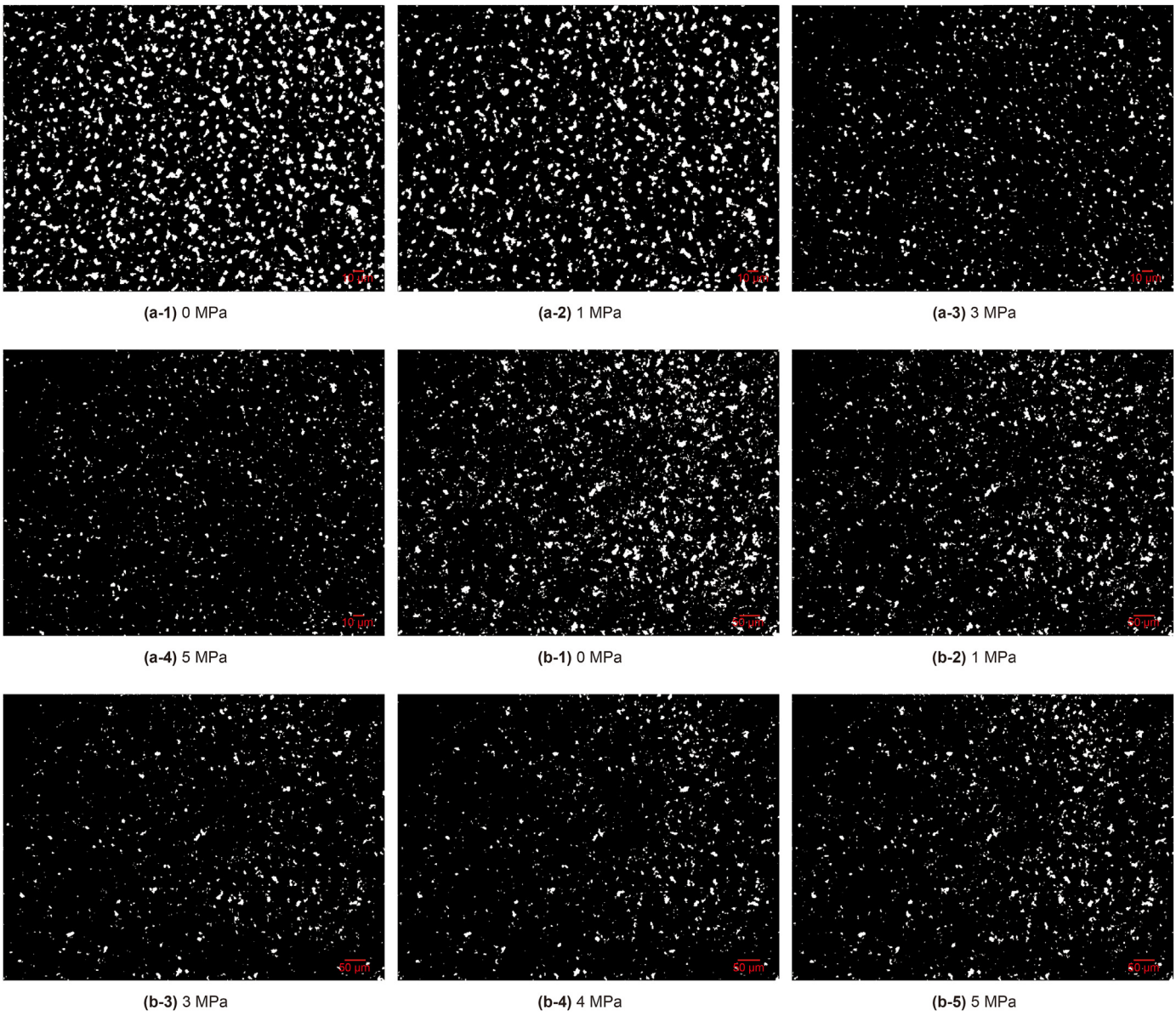

Fig. 11. a Morphology and structure of Shengli crude oil wax crystals under different dissolved gas pressures (30 °C). (**a-1**) 0 MPa. (**a-2**)1 MPa. (**a-3**) 3 MPa. (**a-5**)5 MPa **b** Morphology and structure of Nanyang crude oil wax crystals under different dissolved gas pressures (35 °C). (**b-1**) 0 MPa. (**b-2**)1 MPa. (**b-3**) 3 MPa. (**b-4**)4 MPa. (**b-5**)5 MPa.

Table 4
Wax crystal structure parameters and viscosity at 10 s^{-1} of crude oil under different dissolved gas pressure.

Oil sample	Temperature	Parameters	0 MPa	1 MPa	3 MPa	5 MPa	
Shengli	30 °C	Wax precipitation area, %	18.12	14.4	5.5	3.66	
		Number of particles	1415	1367	1265	1171	
		Average diameter of particles, um	3.798	3.444	2.213	1.876	
		Roundness	0.826	0.841	0.902	0.915	
		Apparent viscosity, Pa·s	8.055	7.606	7.170	6.761	
Oil sample	Temperature	Parameters	0	1	3	4	5
Nanyang	35 °C	Wax precipitation area, %	8.69	6.68	3.75	4.84	5.68
		Number of particles	2078	1850	1099	1318	1410
		Average diameter of particles, um	3.069	2.852	2.772	2.876	3.012
		Roundness	0.848	0.866	0.893	0.886	0.877
		Apparent viscosity, Pa·s	28.016	26.518	24.157	24.424	25.742

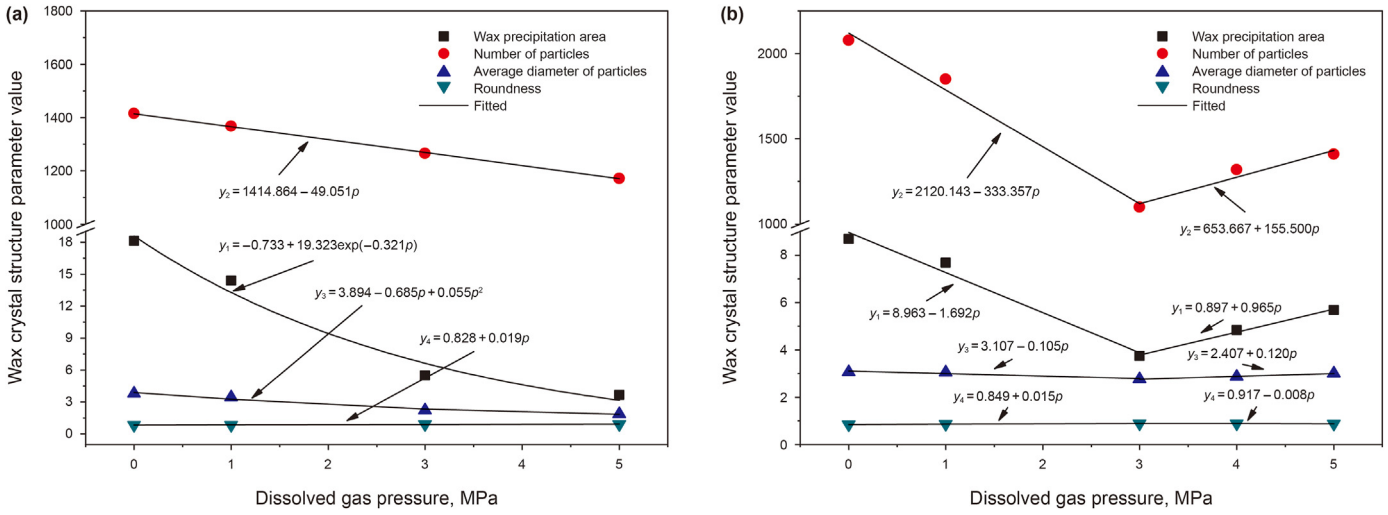

Fig. 12. Relationship between wax crystal structure parameters and dissolved gas pressure. (**a**) Shengli crude oil. (**b**) Nanyang crude oil.

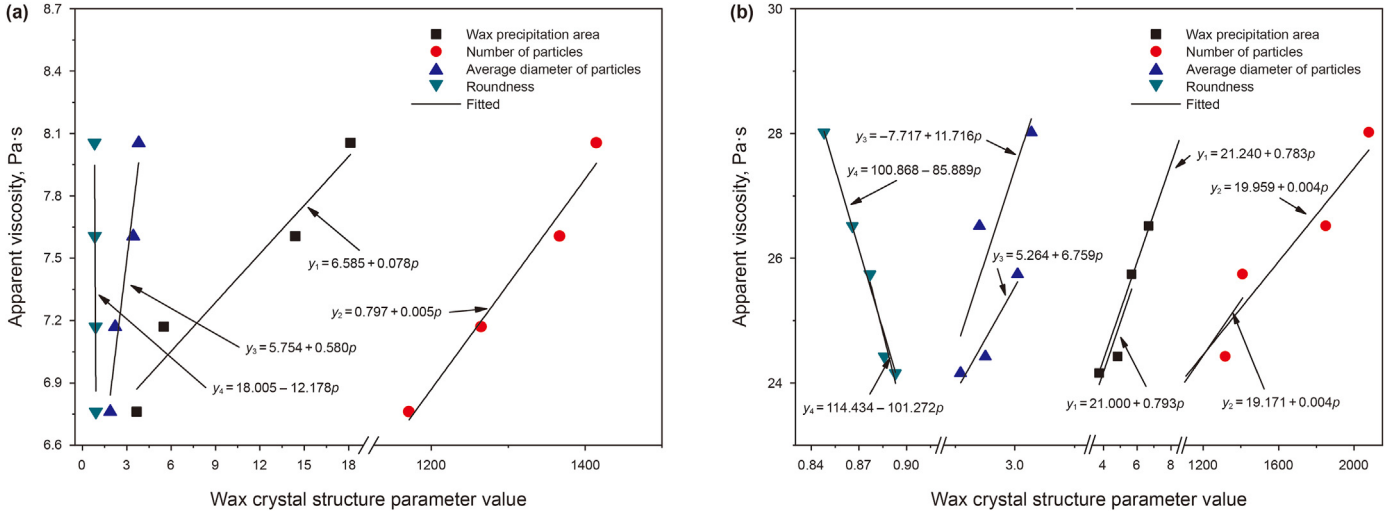

Fig. 13. Relationship between wax crystal structure parameters and apparent viscosity. (**a**) Shengli crude oil. (**b**) Nanyang crude oil.

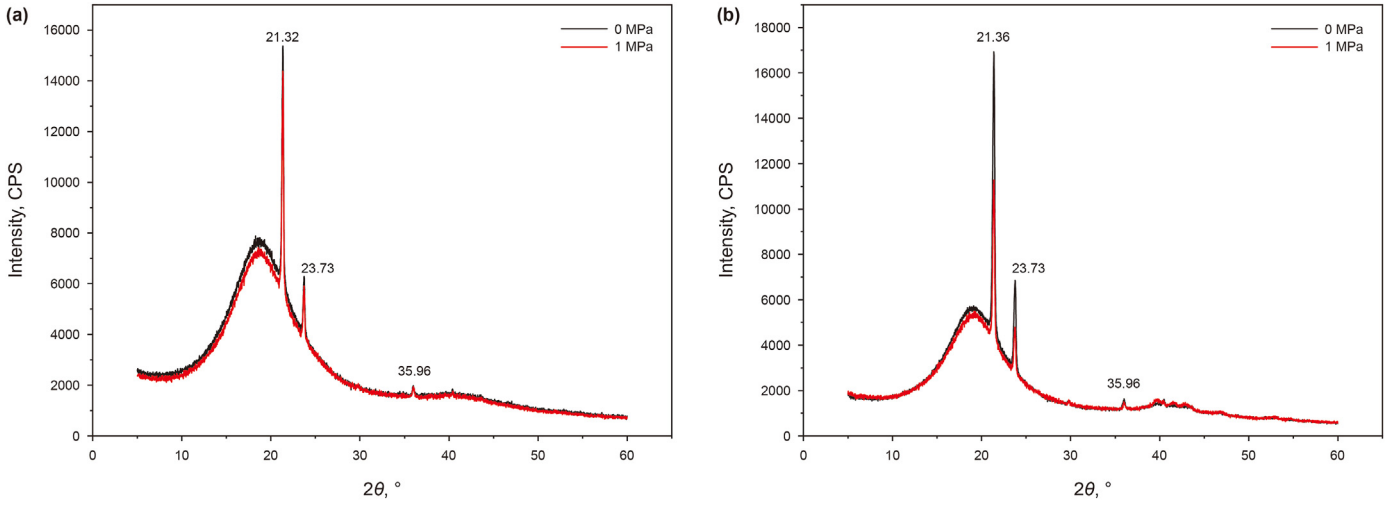

Fig. 14. X-ray diffraction results before and after gas dissolution of crude oil. (**a**) Shengli crude oil. (**b**) Nanyang crude oil.

Table 5
Main diffraction peak data in XRD before and after gas dissolution of crude oil.

Oil sample	2θ/°		Interplanar spacing/nm		Diffraction peak intensity/CPS		Integral strength	
	Degassed crude	Dissolved gas crude oil	Degassed crude	Dissolved gas crude oil	Degassed crude	Dissolved gas crude oil	Degassed crude	Dissolved gas crude oil
Shengli	21.32	21.33	4.17	4.16	15380	14387	60421	30353
	23.73	23.73	3.75	3.74	6287	5909	9585	8026
	35.96	35.95	2.50	2.49	1982	1855	2599	2472
Nanyang	21.36	21.36	4.16	4.15	16930	11288	137120	35853
	23.73	23.73	3.75	3.74	6846	4780	13324	8207
	35.96	35.96	2.50	2.49	1580	1501	2762	2150

4. Conclusion

(1) In summary, the high-pressure microscopic visualization device was developed and designed to observe wax crystals of the dissolved gas in Shengli and Nanyang crude oil.
(2) The change in the rheology of crude oil was resulted in comprehensive influence of the pressure caused by CH_4 dissolution.
(3) The dissolution of CH_4 affected the non-isothermal crystallization process of crude oil, i.e. the wax precipitation point of Shengli crude oil showed different wax precipitation behavior in the counterpart of Nanyang crude oil. The CH_4 dissolution improved the solubility of crude oil to wax, and the existence of CH_4 molecules hindered the formation of wax crystals that reduced the wax precipitation point of crude oil. However, the pressure caused by the dissolved gas led to the compression and aggregation of crude oil molecules that limited the solubility of wax molecules in liquid oil, and consequently, the wax precipitation temperature of crude oil increased.
(4) The wax precipitation area, number of particles, and average diameter of particles of crude oil gradually decreased due to the CH_4 dissolution. As the dissolved gas was gradually saturated in oils, wax crystals formed a linked network, resulted in a big size of the wax crystal. Through the analysis of wax crystal images, it was confirmed that CH_4 dissolution affected the shape of wax crystal particles, effective internal phase volume fraction, and flocculation capacity of wax crystal flocs, showing a changing rheology of crude oil.
(5) The XRD curves of Shengli and Nanyang crude oil showed an unchanged crystal structure before and after the CH_4 dissolution. It can be verified that CH_4 dissolution affected the rheology of oil by means of the wax crystallization process, crystallization ability, and morphology of wax crystal. The dissolved gas caused compact wax crystal structure in both oil samples. In the process of wax crystal growth, the crystal surface was destroyed, the main characteristic diffraction peak intensity of wax crystal and the grain size of wax crystal decreased. At the same time, the area density of plane 110 and the size of wax crystal decreased greatly.

Acknowledgements

The authors are grateful to the National Natural Science Foundation of China (51774315, 51574274), the Natural Science Found of Hebei Province (E2020203013) for the support of this work.

References

Abivin, P., Henaut, I., Moan, M., et al., 2008. Rheological characterization of foamy oils under pressure. Am. Inst. Phys. 1027, 827–829. https://doi.org/10.1063/1.2964861.
Agarwal, J.R., Torres, C.F., Shah, S., 2021. Development of dimensionless parameters and groups of heat and mass transfer to predict wax deposition in crude oil pipelines. ACS Omega 6 (16), 10578–10591. https://doi.org/10.1021/acsomega.0c05966.
Bank, G.C., Riestenberg, D.E., Koperma, G.J., 2007. CO_2-enhanced Oil Recovery Potential of the Appalachian Basin. Eastern Regional Meeting. https://doi.org/10.2523/111282-MS.
Bao, Y.Q., Zhang, J.J., Wang, X.Y., et al., 2016. Effect of pre-shear on structural behavior and pipeline restart of gelled waxy crude oil. RSC Adv. 6 (84), 80529–80540. https://doi.org/10.1039/C6RA16346G.
Chen, X., Sun, G., Liu, D., et al., 2021. Two effects of wax crystals on stabilizing water-in-oil emulsions. Colloids Surf. A Physicochem. Eng. Asp. 625, 126884. https://doi.org/10.1016/j.colsurfa.2021.126884.
Cheng, C., Bogerr, D.V., Nguyen, Q.D., 2000. Influence of thermal history on the waxy structure of statically cooled waxy crude oil. SPE J. 5 (2), 148–156. https://doi.org/10.2118/57959-pa.
Fakroun, A., Benkreira, H., 2019. Rheology of waxy crude oils in relation to restart of gelled pipelines. Chem. Eng. Sci. 211 (2), 115212. https://doi.org/10.1016/j.ces.2019.115212.
Garcia, M.D.C., Carbognani, L., 2001. Asphaltene-paraffin structural interactions. Effect on crude oil stability. Energy Fuels 15, 1021–1027. https://doi.org/10.1021/ef0100303.
Hinai, N.M.A., Myers, M.B., Dehghani, A.M., et al., 2019. Effects of oligomers dissolved in CO_2 or associated gas on IFT and miscibility pressure with a gas-light crude oil system. J. Petrol. Sci. Eng. 181, 106210. https://doi.org/10.1016/j.petrol.2019.106210.
Hou, L., Jia, L., Liu, J., 2014. Experimental research on the wax crystal particle size distribution of waxy crude oil. Petrol. Sci. Technol. 32 (17), 2137–2142. https://doi.org/10.1080/10916466.2013.769573.
Hu, R., Crawshaw, J.P., Trusler, J.P.M., et al., 2017. Rheology and phase behavior of carbon dioxide and crude oil mixtures. Energy Fuels 31 (6), 5776–5784. https://doi.org/10.1021/acs.energyfuels.6b01858.
Huang, Q.Y., Wang, L., 2013. Effect of droplet distribution on rheological properties of water-in-oil emulsion in waxy crude oils. Acta Pet. Sin. 34 (4), 765–774 (in Chinese).
Jing, J.Q., Lu, P., Li, Y., et al., 2008. Wax crystal fractal characteristics of Daqing crude oil before and after adding flow improver. J. Southwest Petrol. Univ. (Sci. & Technol. Ed.) 30 (20), 123–126 (in Chinese).
Li, B.F., Liu, G., Xing, X., et al., 2019a. Molecular dynamics simulation of CO_2 dissolution in heavy oil resin-asphaltene. J. CO_2 Util. 33, 303–310. https://doi.org/10.1016/j.jcou.2019.06.011.
Li, B.F., Liu, G., Ren, S.Y., et al., 2019b. Non-isothermal crystallization kinetics of waxy crude oil. Petrol. Sci. Technol. 37 (3), 282–289. https://doi.org/10.1080/10916466.2018.1539755.
Li, C.X., 2007. Rheology of Crude Oil. China University of Petroleum Press (in Chinese).
Li, H., Zhang, J., Xu, Q., et al., 2020. Influence of asphaltene on wax deposition: deposition inhibition and sloughing. Fuel 266, 117047. https://doi.org/10.1016/j.fuel.2020.117047.
Li, Y., Zhao, J., Dong, H., et al., 2021. The role of shearing effect in the evolution of the microscopic behavior of wax crystals. New J. Chem. 45, 10418–10431. https://doi.org/10.1039/D1NJ01407B.
Liu, G., Zhang, L.P., Zhang, G.Z., et al., 2010. Fractal characteristics of Nanyang waxy crude oil. J. China Univ. Petrol. (Ed. Natl. Sci.) 34 (3), 109–112 (in Chinese).
Liu, L., Pu, X., Zhou, Y., et al., 2020. Phase inversion of pickering emulsions by electrolyte for potential reversible water-in-oil drilling fluids. Energy Fuels 34 (2), 1317–1328. https://doi.org/10.1021/acs.energyfuels.9b03117.
Magda, J.J., El-Gendy, H., Oh, K., et al., 2009. Time-dependent rheology of a model waxy crude oil with relevance to gelled pipeline restart. Energy Fuels 23 (2), 1311–1315. https://doi.org/10.1021/ef800628g.
Oliveira, G.E., Mansur, C.R.E., Lucas, E.F., et al., 2007. The effect of asphaltenes, naphthenic acids, and polymeric inhibitors on the pour point of paraffins solutions. J. Dispersion Sci. Technol. 28 (3), 349–356. https://doi.org/10.1080/01932690601107526.
Saboorian, J.H., 2012. A novel methodology for simultaneous estimation of gas diffusivity and solubility in bitumens and heavy oils. In: SPE Heavy Oil Conference Canada. Society of Petroleum Engineers. https://doi.org/10.2118/157734-MS.
Yang, F., Li, C.X., Li, B., et al., 2014. The solubility and rheology of live oils saturated

by different alkane gases. Petrol. Sci. Technol. 32 (11), 1340–1348. https://doi.org/10.1080/10916466.2012.656870.
Yang, F., Zhu, H., Li, C., et al., 2021. Investigation on the mechanism of wax deposition inhibition induced by asphaltenes and wax Inhibitors. J. Petrol. Sci. Eng. 204 (7), 108723. https://doi.org/10.1016/j.petrol.2021.108723.
Yang, Z.H., Li, M.Y., Peng, B., et al., 2012. Dispersion property of CO_2 in oil. 1. volume expansion of CO_2+alkane at near critical and supercritical condition of CO_2. J. Chem. Eng. Data 57 (3), 882–889. https://doi.org/10.1021/je201114g.
Yang, Z.H., Li, M.Y., Peng, B., et al., 2013. Volume expansion of CO_2+oil at near critical and supercritical conditions of CO_2. Fuel 112 (10), 283–288. https://doi.org/10.1016/j.fuel.2013.04.037.
Yi, S.Z., Zhang, J.J., 2011. Shear-Induced change in morphology of wax crystals and flow properties of waxy crudes modified with the pour-point depressant. Energy Fuels 25 (12), 5660–5671. https://doi.org/10.1021/ef201187n.
Yokozeki, A., 2007. Solubility correlation and phase behaviors of carbon dioxide and lubricant oil mixtures. Appl. Energy 84 (2), 159–175. https://doi.org/10.1016/j.apenergy.2006.05.003.
Yu, T., 2009. Study on Rheological Properties of Dissolved Gas Crude Oil. China University of Petroleum (East China) (in Chinese).
Yu, L., Li, S., Stubbs, L.P., et al., 2021. Rheological investigation of clay-stabilized oil-in-water Pickering emulsions for potential reservoir applications. J. Petrol. Sci. Eng. 204 (21), 108722. https://doi.org/10.1016/j.petrol.2021.108722.
Zhang, L.P., 2011. Study on Microscopic Characteristic of Waxy Crude Oil. China University of Petroleum (East China) (in Chinese).